Covalent modification of calcium hydroxy and fluoroapatite surface by grafting alkylphosphonate

Hassen Agougui, Abdallah Aissa, Mongi Debbabi*

Laboratoire de Physico-Chimie des Matériaux, Faculté des Sciences de Monastir, 5019 Monastir, Tunisia

*corresponding author.Tel. : +216 98 439 692

E-mail: m.debbabi@yahoo.fr

Calcium hydroxyl and fluoroapatite (CaHAp and CaFAp) were prepared in the presence of the 2-carboxyletylphosphonic acid (2-CEPA), by hydrothermal method. The incorporation of phosphonic acid within the apatite structure was confirmed by powder XRD, IR and MAS-NMR spectroscopies and SSA. The X-ray powder analysis showed that the cristallinity was not affected by the presence of organic moieties. IR spectroscopy showed new vibration modes related to phosphonate groups. ^{31}P MAS-NMR spectra exhibit new signals, assigned to the presence of organic phosphorus. Specific surface area (SSA) increases with increasing of phosphonate amount, especially for CaHAp. According to these results, a mechanism is proposed for the formation of two types of ionic interaction (-C-O-Ca) and (Ca-O-P_{org}).

Key words: Surface modification, phosphonate, hydrothermal method.

I. INTRODUCTION

The adsorption of macromolecules on the surface of apatite has been the subject of much research (Tanaka *et al.*, 2004). The interaction between the apatite surface and molecules is related to various surface properties (surface functional groups, acidity and basicity, surface charge, hydrophilicity and porosity) (Pramanik *et al.*, 2009). The grafted compounds can be linked on the apatitic surface by covalent bond or electrostatic interaction (Kandori *et al.*, 1999). The phosphonate–apatite hybrids obtained have interesting applications due to the combination of some characteristic properties of apatite (mechanical and chemical properties, exchange capacity, bioreactivity, optical properties) with those of the phosphonate (polymerization, stability over wide ranges of pHs and temperatures). Such applications are in various fields; catalysis (Zahouily *et al.*, 2005), chromatography (Liu *et al.*, 1998) and biomedical (Fukegawa *et al.*, 2006). The aim of this work is to study the synthesis of CaHAp and CaFAp by hydrothermal method, in the presence of alkylphosphonate (2-CEPA), in order to compare the reactivity of CaHAp and CaFAp.

II. EXPERIMENTAL

CaHAp and CaFAp were synthesized by adding a 0.75 M calcium nitrate solution (15 ml) and 0.25 M diammonium hydrogen phosphate solution (25 mL) + NH_4F (for CaFAp) into a flask containing a dilute solution of ammonium hydroxide in order to keep the pH above nine during precipitation. The reactions were carried out at room temperature under stirring and nitrogen stream. The obtained solution was treated in autoclave (V = 60 mL) under hydrothermal conditions at 120 °C, for 15 h. The products were filtered, washed and dried overnight at 100 °C. Grafted (CaHAp-CaFAp)/(2-CEPA) was obtained following a similar procedure except for the phosphorus containing solutions that were prepared by mixing (1−x) moles of $(NH_4)_2HPO_4$ with x mol (x = 0.05, 0.1 and 0.2) of (2-CEPA).

III. CHARACTERIZATION TECHNIQUES

III.1.Xray powder diffraction analysis

X-ray powder diffraction was used for phase analysis of the synthesis samples. The analysis was carried out with a Panalytical X'Pert PRO MPD equipped with copper anticathode tube. The diffraction spectra were recorded in the range from 10 to 80 with a step of and a step duration of 0.92 s.

https://doi.org/10.1017/S0885715613001048 Published online by Cambridge University Press

III.2. Chemical analysis

The calcium and phosphorus contents were obtained by ICP-OES on a Horiba jobin yvon modele activa. The chemical analysis of the carbon has been determined according to the Anne method (Anne, 1945).

III.3. Infrared spectroscopy

The IR spectra were recorded on a Bio-Rad FTS FT-IR spectrophotometer as KBr pellets in the 4000–400 cm^{-1} region.

III.4. MAS-NMR spectroscopy

Solid-state ^{31}P MAS NMR spectra were recorded at 121.5 MHz on a Bruker spectrometer Advanced 300 (rotor 4mm, spinning rate 2-12 KHz).

IV. RESULTS AND DISCUSSIONS

IV. 1. Elemental analysis

The results of chemical analysis, specific surface area (SSA), pore volume V_p and mean pore diameter D_p for hydroxy- and fluorapatites before and after modification by 2-CEPA are reported in Table I.

Table I**:** Chemical composition (±0.02) of hydroxy-fluoroapatite before and after reaction with 2-carboxylethyl phosphonic acid.

Sample	%C	Ca/P	SSA(m^2/g)	V_p (cm^3 g^{-1})	D_p (Å)
CaHAp	0.12	1.61	54.83	4.87810^{-3}	110.20
CaHAp-(2-CEPA)10	1.02	1.60	190.90	5.04610^{-4}	126.80
CaHAp-(2-CEPA)20	1.40	1.59	236.10	8.61810^{-3}	123
CaFAp	0.05	1.65	56.22	1.61110^{-3}	120.7
CaFAp-(2-CEPA)10	0.45	1.62	104.3	$6.54\ 10^{-3}$	117.6
CaFAp-(2-CEPA)20	0.61	1.61	151.8	$5.169\ 10^{-3}$	122.2

For all modified phases, the percentages of carbon and SSA increases with increasing of the grafting rate of (2-CEPA). These obtained values are distinctly superior for CaHAp compared to CaFAp. The maximum value of SSA is obtained for CaHAp-(2-CEPA) (x=20%).

https://doi.org/10.1017/S0885715613001048 Published online by Cambridge University Press

IV. 2. IR spectroscopy

IR spectra of CaHAp and CaFAp, as well are those of the modified apatites, present the characteristic bands of $(PO_4)^{3-}$ groups (Figures 1 and 2): (ν_s) (963 cm^{-1}), (δ_s) (477 cm^{-1}), (ν_{as}) (1040-1095 cm^{-1}) and (δ_{as}) (568-604 cm^{-1}). Moreover, characteristic bands of hydroxyl ions are observed towards 3572 cm^{-1}(ν_s) and 630 cm^{-1}(ν_L) for CaHAp. For samples synthesized in the presence of 2-CEPA, new peaks characteristics of organic moieties are observed such as $\delta_{(CH2)}$ (743 cm^{-1}), $\upsilon_{(COO-)}$ (872, 1568 cm^{-1}) and $\upsilon_{(CH)}$ 2929 cm^{-1}. These bands are more intense for CaHAp-(2-CEPA) (x=20%). On the other hand, the intensity of the hydroxyl bands (υ_s at 3577 cm^{-1}) and (υ_L at 636 cm^{-1}) decreases progressively with increasing of 2-CEPA concentration. This phenomenon can be explained by the replacement of hydroxyl ions in apatitic structure by (2-CEPA).

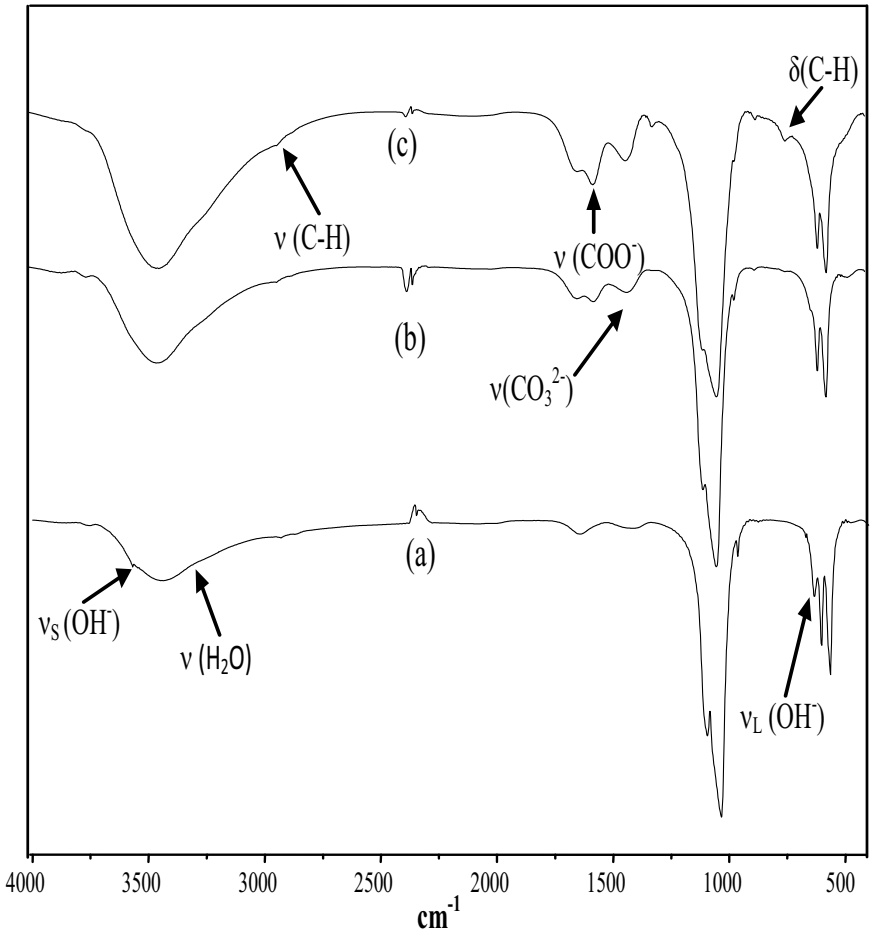

Figure 1: IR spectra of CaHAp: ungrafted (a); CaHAp-(2-CEPA)10 (b) and CaHAp-(2-CEPA)20 (c).

https://doi.org/10.1017/S0885715613001048 Published online by Cambridge University Press

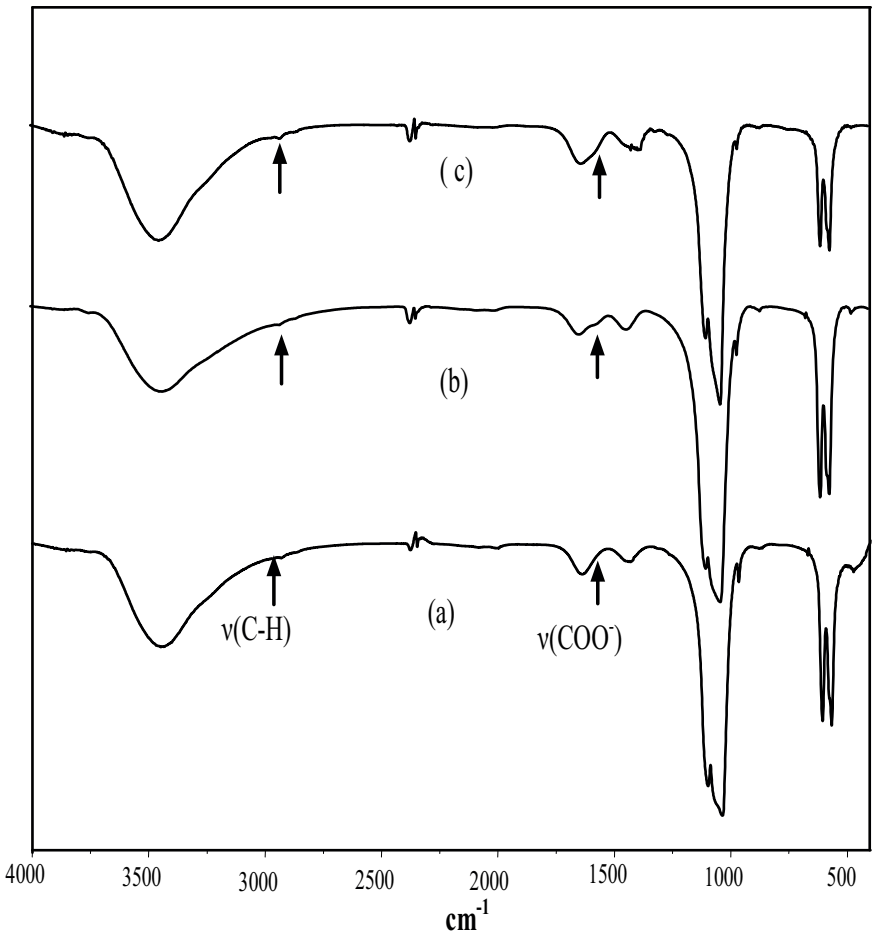

Figure 2: IR spectra of CaFAp: ungrafted (a); CaFAp-(2-CEPA)10 (b) and CaFAp-(2-CEPA)20 (c).

IV. 3. X-ray diffraction

XRD patterns of all products prepared are represented in Figures 3 and 4. Preliminary analysis of these diagrams shows that the apatitic structure remains unchanged after treatment with different amounts of phosphonate and no other crystalline phase was detected. All compounds are single-phase. Moreover, the increasing of phosphonate concentration in the starting solution leads to the decrease of the material crystallinity as shown by the broadening of the peaks and the decrease of their intensities.

The influence of the grafting rate on the evolution of the crystallite size *D* can be evaluated for the (002) and (310) reflections. The values of *D* were calculated using the Debye-Scherrer equation (Bigi *et al.*, 2007):

$$D = \frac{K\lambda}{\beta_{1/2}\cos\theta}$$

https://doi.org/10.1017/S0885715613001048 Published online by Cambridge University Press

Where λ is the wavelength, θ is the diffraction angle, K is a fixed constant equal to 0.9 for apatite crystallites and $\beta_{1/2}$ is the full width at half maximum intensity (FWHM) a given reflection. The crystallinity is defined as the fraction of the crystalline phase in the total mass of apatite and is noted as X_c . For the evaluation of crystallinity, an empirical relation between X_c and $\beta_{1/2}$ is commonly deduced according to the following equation (Ren *et al.*, 2009).

$$X_c = (K_A/ \beta_{1/2})^3$$

where K_A is a constant set at 0.24 for the case of apatite and $\beta_{1/2}$ is the FWHM of the (002) reflections.

The results are summarized in Table II. The decrease in the crystallite size and crystallinity is regular in function of increase in the rate of grafting. However, this decrease is less remarkable in the case of fluorapatite.

Table II**.** Crystal sizes (D_{hkl}) evaluated from the width at half maximum intensity of the (002) and (310) reflections of ungrafted and grafted apatite.

Sample	**$\beta_{1/2}$(002)(°)**	**D_{002}(Å)**	**$\beta_{1/2}$(310)(°)**	**D_{310}(Å)**	**Crystallinity (Xc)**
CaHAp	0.164	497	0.421	201	3.131
CaHAp-(2-CEPA)10	0.343	238	0.956	88	0.343
CaHAp-(2-CEPA)20	0.530	154	1.850	46	0.092
CaFAp	0.206	407	0,258	328	1.581
CaFAp-(2-CEPA)10	0.315	259	1.084	78	0.440
CaFAp-(2-CEPA)20	0.338	241	1.44	59	0.357

https://doi.org/10.1017/S0885715613001048 Published online by Cambridge University Press

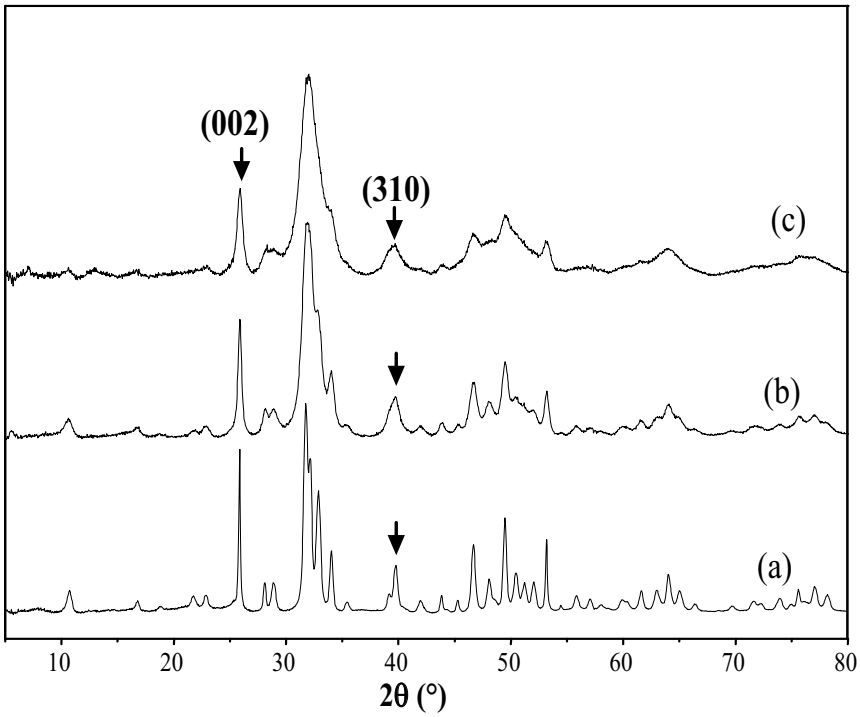

Figure 3: X-ray powder diffraction pattern of CaHAp before and after modification by grafting (2-CEPA): ungrafted (a); CaHAp-(2-CEPA)10 (b) and CaHAp-(2-CEPA)20 (c).

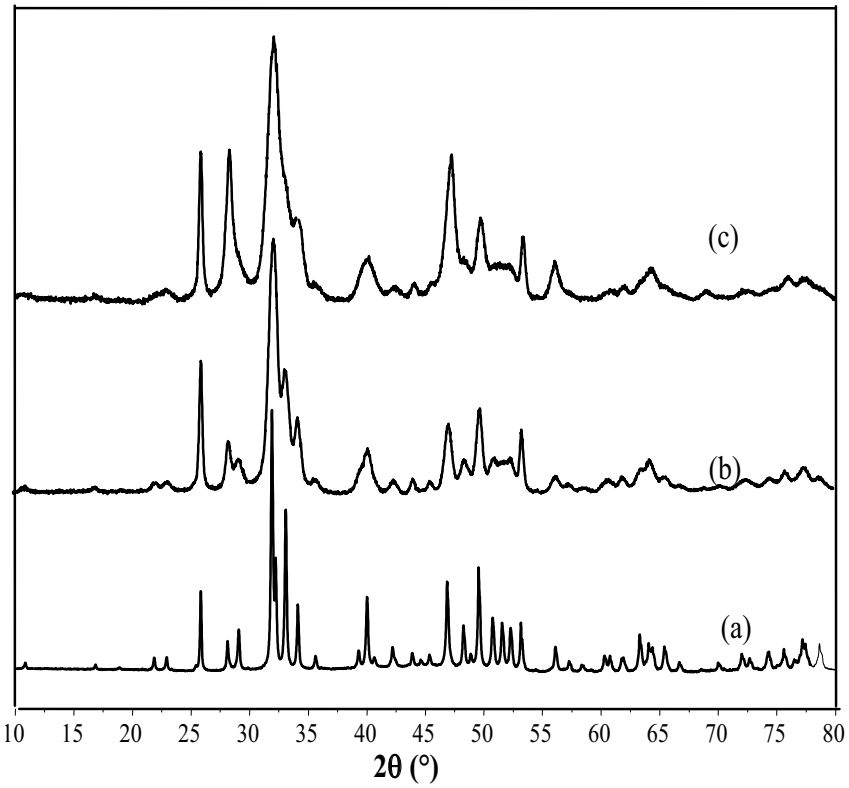

Figure 4: X-ray powder diffraction pattern of CaFAp before and after modification by grafting (2-CEPA): ungrafted (a); CaFAp-(2-CEPA)10 (b) and CaFAp-(2-CEPA)20 (c).

https://doi.org/10.1017/S0885715613001048 Published online by Cambridge University Press

The indexing of diffraction patterns in the hexagonal system and space group *P63/m* for the different phases allowed us to determine the lattice parameters, calculated using the software EXPO 2009 (Altomare *et al.*, 2009) and the results are listed in Table III.

Table III: The unit cell parameters of CaHAp and CaFAp before and after grafting by (2-CEPA).

Sample	a (Å)	c (Å)
CaHAp	9.4156(8)	6.8758(2)
CaHAp-(2-CEPA)10	9.446(5)	6.891(2)
CaHAp-(2-CEPA)20	9.477(4)	6.866(4)
CaFAp	9.360(1)	6.877(2)
CaFAp-(2-CEPA)10	9.375(8)	6.888(4)
CaFAp-(2-CEPA)20	9.401(3)	6.911(3)

For all grafted fluoroapatites by (2-CEPA), *a* and *c* lattice parameters varied slightly. Contrariwise, for the modified hydroxyapatite, the increase of *a* parameter is more significant. This result can confirm the hypothesis in the IR spectroscopy concerning the replacement of OH^- in apatitic structure by (2-CEPA). From these results we proposed a model (Scheme 2) gives us an idea about the fixation of (2-CEPA) in tunnel. (2-CEPA) acid are introduced in tunnels following c axis.The crystallites are developed along the a and b axes.

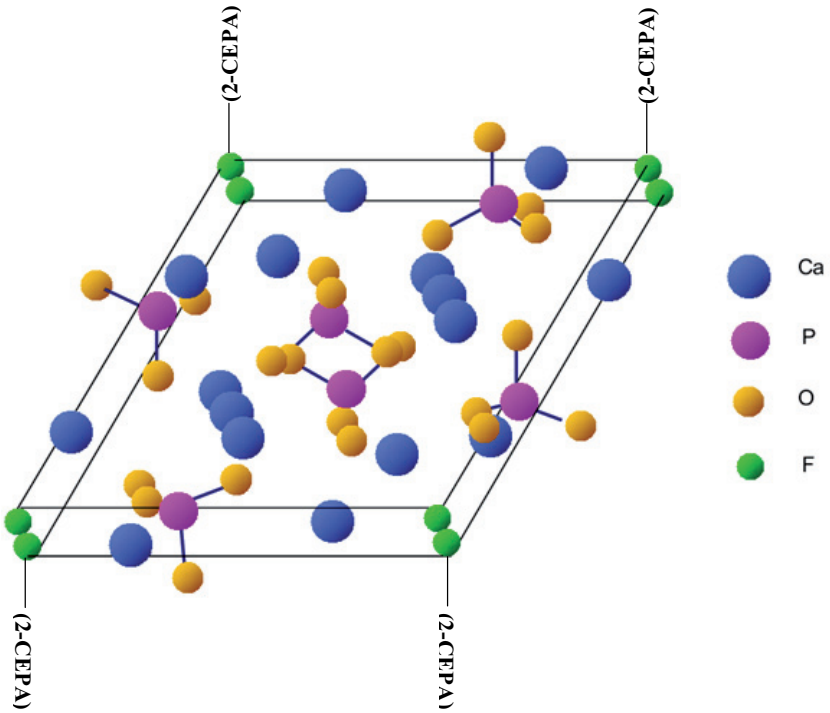

Scheme 1. The proposed mechanism for reaction between (2-CEPA) and CaHAp or CaFAp.

https://doi.org/10.1017/S0885715613001048 Published online by Cambridge University Press

IV. 4. MAS-NMR spectroscopy

IV. *4.1.* ^{31}*P CP-MAS NMR*

For ungrafted apatite an isotropic ^{31}P NMR signal is observed around +2.8 ppm corresponding to the $(PO_4)^{3-}$ anion, whereas the ^{31}P NMR of 2-CEPA shows the presence of an isotropic signal at 30.65 ppm. For all grafted phases (Figures 5 and 6), a broadening of the isotropic signal was observed and related to the heterogeneity of phosphorus environment. In presence of 2-CEPA two additional signals are obtained at 25 and 34 ppm, due to the double acidic functions of the organic reactant (carboxylic and phosphonic acidities). These data indicate that 2-CEPA can establish two kinds of bonds with the apatite by the two different hydroxyl groups -C-OH or -P-OH (scheme 2). These results clearly show the reactivity of 2-CEPA towards Ca^{2+} by formation of two ionic bonds Ca-O-C (34 ppm) and Ca-O-P_{org} (25 ppm) (Agougui *et al.*, 2010).

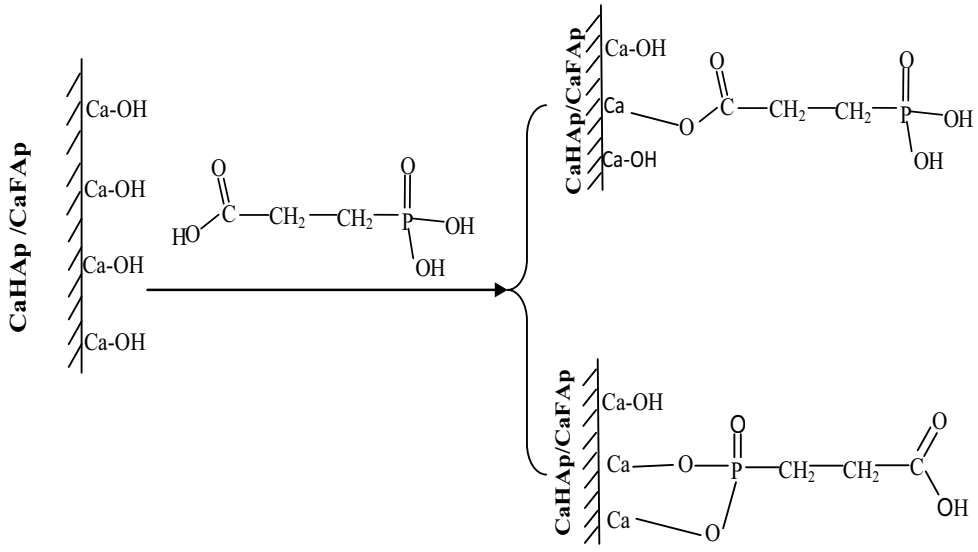

Scheme 2. The proposed model for the fixation of (2-CEPA) in tunnel.

https://doi.org/10.1017/S0885715613001048 Published online by Cambridge University Press

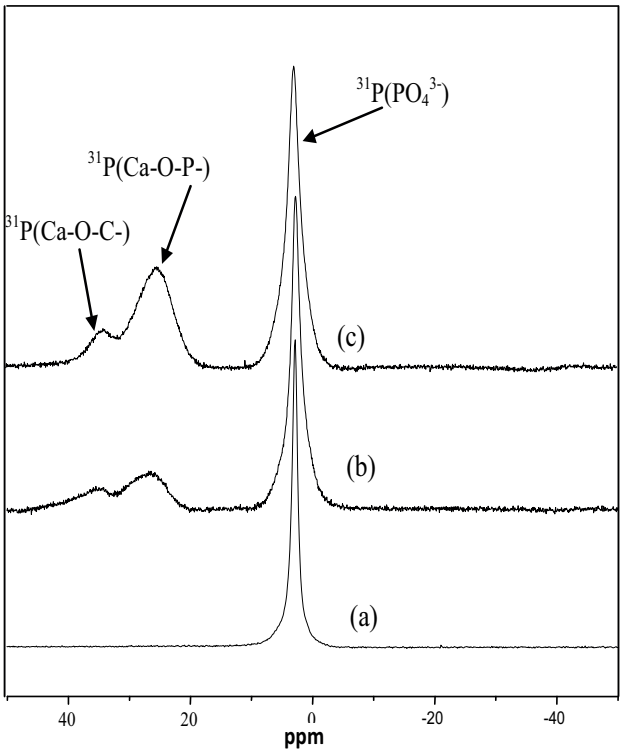

Figure 5 : ^{31}P CP/MAS-NMR spectra of CaHAp before and after surface modification by grafting (2-CEPA): ungrafted (a); CaHAp-(2-CEPA)10 (b) and CaHAp-(2-CEPA)20 (c).

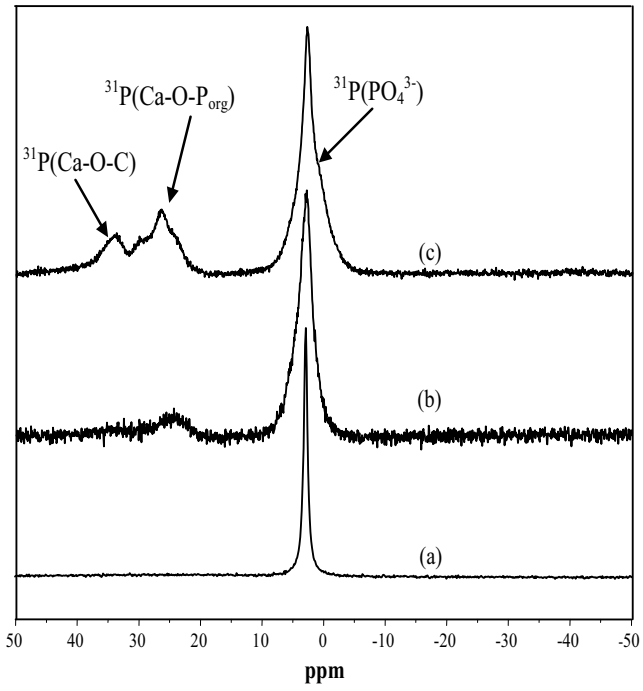

Figure 6: ^{31}P CP/MAS-NMR spectra of CaFAp before and after surface modification by grafting (2-CEPA): ungrafted (a); CaFAp-(2-CEPA)10 (b) and CaFAp-(2-CEPA)20 (c).

https://doi.org/10.1017/S0885715613001048 Published online by Cambridge University Press

The percentage of Ca-O-P_{org} bond is higher than Ca-O-C-. These percentages are notably larger for CaHAp grafted than for CaFAp (Table IV).

Table IV: Chemical shift δ_{iso} of CaHAp and CaFAp before and after reaction with (2-CEPA).

Sample	Spectra	δ_{iso}±0.1(ppm)	% (Ca-O-P_{org})	$\Delta_{1/2}$	% (Ca-O-C-)
CaHAp	^{31}P	2.85	-	0.91	-
CaFAp	^{31}P	2.87	-	0.74	-
CaHAp-(2-CEPA)10	^{31}P-^{1}H	2.81; 5.30; 25.25; 33.80	27.58	2.01; 1.72; 5.86; 4.67	7.72
CaHAp-(2-CEPA)20	^{31}P-^{1}H	2.87; 5.11; 25.31; 33.95	39.87	2.51; 1.41; 7.72; 3.93	8.05
CaFAp-(2-CEPA)10	^{31}P-^{1}H	3.08; 24.77; 33.78	10.27	2.67; 4,31; 10.76	8.60
CaFAp-(2-CEPA)20	^{31}P-^{1}H	0.22; 2.77; 26.41; 34.24	22.22	2.65; 2,51; 4.15; 5.22	14.95

V. CONCLUSION

New hybrid compounds CaHAp-2-CEPA) or CaFAp-(2-CEPA) were prepared by hydrothermal method. The reaction of (2-CEPA) with CaHAp and CaFAp is effective and leads to incorporation of phosphonate moiety in the apatitic structure. Therefore, all characterization techniques show that the CaHAp is more reactive than of CaFAp. According to ^{31}P NMR studies, apatite modified by grafting (2-CEPA) leads to the formation of organometallic bond Ca-O-Porg and Ca-O- C-.

Agougui, H., Aissa, A., Maggi, S. and Debbabi, M. (**2010**). "Phosphonate-Hydroxyapatite hybrid compounds prepared by hydrothermal method," Appl. Surf. Sci. **257**, 1377–1382.

Altomare, A., Camalli, M., Cuocci, C., Giacovazzo, C., Moliterni, A. and Rizzi, R. (**2009**). "*EXPO2009*: structure solution by powder data in direct and reciprocal space," J. Appl. Crystallogr. **42**, 1197–1202.

Anne, P. **(1945)**. "Sur le dosage rapide du carbone organique de sols," Ann. Agron. **15**, 161–172.

Bigi, A., Boanini, E., Capuccini, C. and Gazzano, M. (**2007**). "Strontium-substituted hydroxyapatite nanocrystals," Inorg. Chim. Acta **360**, 1009–1016.

https://doi.org/10.1017/S0885715613001048 Published online by Cambridge University Press

Fukegawa, D., Hayakawa, S., Yoshida, Y., Suzuki, K., Osaka, A. and Van Meerbeek, B. (**2006**). "Chemical Interaction of Phosphoric Acid Ester with Hydroxyapatite," J. Dent. Res. **85**, 941–944.

Liu, Q., de Wijn, J. R., de Groot, K. and van Blitterswijk, C. A. (**1998**). "Surface modification of nano-apatite by grafting organic polymer," Biomaterials **19**, 1067–1072.

Kandori, K., Fujiwara, A., Yasukawa, A. and Ishikawa, T. (**1999**). "Preparation and characterization of hydrophobic calcium hydroxyapatite particles grafting oleylphosphate groups," Colloids Surf., A **150**, 161–170.

Pramanik, P., Mohapatra, N. and Bhargava, S. (**2009**). "Chemical synthesis and characterization of hydroxyapatite (HAp)-poly (ethylene co vinyl alcohol) (EVA) nanocomposite using a phosphonic acid coupling agent for orthopedic applications," Mater. Sci. Eng., C **29**, 228–236.

Ren, F., Xin, R., Ge, X. and Leng, Y. (**2009**). "Characterization and structural analysis of zinc-substituted hydroxyapatites," Acta Biomater. **5**, 3141–3149.

Tanaka, H., Futaoka, M. and Hino, R. (**2004**). "Surface modification of calcium hydroxyapatite with pyrophosphoric acid," J. Colloid Interface Sci. **269**, 358–363.

Zahouily, M., Bahlaouan, W., Bahlaouan, B., Rayadh; A. and S, Sebti. (**2005**). "Catalysis by hydroxyapatite alone and modified by sodium nitrate," Arkivoc. **xiii**, 150–161.

https://doi.org/10.1017/S0885715613001048 Published online by Cambridge University Press